Journal of Engineering and Applied Sciences 13 (12): 4305-4313, 2018
ISSN: 1816-949X

Numerical Analysis of Various Parameters on the Dynamics of Drop Formation

Pardeep Bishnoi and M.K. Sinha
National Institute of Technology, Department of Mechanical Engineering,
Jamshedpur, 831014 Jharkhand, India

Abstract: This research validates the computational results regarding the effects of viscosity, the flow rate on the dynamics of drop formation in the continuous jetting mode with the experimental results available in the literature. In this research, volume of fluid method is used for tracking the droplet during detachment process. Various stages of drop formation including ejection and neck development of liquid thread and its breakoff into primary drops are studied. The deviation of pressure is also analyzed. The variation of the smallest width of thread and thread length is also studied for various time periods. It is also observed that the size of the primary drop increases slightly with the increase in surface tension and decreasing viscosity whereas while the effect of density on the size of the primary drop is negligible. Furthermore, mathematical models using power law, allometric curve and exponential decay function were also constructed. The coefficient of determination also achieved the higher values (0.97-0.99). Drop formation process is widely used in IC engines for atomization purposes in the paint industry and especially in the medical field for determining certain diseases.

Key words: Drop formation, Volume of Fluid (VOF), pendent drop, variation, primary, IC engines

INTRODUCTION

Due to various applications (Basaran, 2002), dynamics of drop formation becomes a topic of interest for research. It is widely used in the extraction process, inkjet printing, spray cooling, etc. In today's life, there are a number of methods (Eggers, 1997; Bhat, 2008) available for producing a drop from a nozzle or capillary tube's orifice. These are dripping, jetting (or continuous jetting), drop on demand and drop layering. Dripping and jetting completely depends on the flow rates. Dripping happens for low flow rate under the gravity force. The breakoff time taken in this case is more as compared to the jetting mode. Continuous jetting mode occurs when there is an increase in the liquid flow rate. This type of drop formation along with some control system is widely used in current printing industry. In the Drop on Demand (DoD), ejection of the drop occurs as per requirement. Inkjet printing process mainly works on DoD method (Doring, 1982). Other than inkjet printing DoD process is being used more and more in several emerging applications such as the formation of three-dimensional biological structures (Calvert, 2007) that are useful in the study of artificial organs and fabrication of polymer transistors (Sirringhaus *et al*., 2000) and solar cells (Rembe *et al*., 1996, 1999).

Dynamic of drop formation depends on various factors like the viscosity of the liquid, surface tension between the liquid and atmospheric medium, density of the liquid, flow rate of the liquid in the capillary tube, etc.

Savart (1833) experimentally observed the drop formation phenomenon when a stream of water flowed through a nozzle as shown in Fig. 1. Small drops in between the two bigger drops named as 'Satellite drop'. He stated from his experimental study that drop formation did not depend on gravity. However, he did not understand the surface tension effects on the drop dynamic which was later observed by Rayleigh (1878). According to Rayleigh, drop formation occurs due to the gravity forces. Different aspects of dripping, jetting, liquid bridge and various stability factors that occur in the drop formation were explained by Egger (1997).

Hauser *et al*. (1936) and Stone *et al*. (1986) pictured the drop detachment process before, during and after the breakup in their experiments. Tjahjadi *et al*. (1992) investigated experimentally, the effect of interfacial tension, viscosity ratio on the satellite drop formation. Wehking (2014) experimentally revealed the effect of the physical and geometric property of the system on the drop dynamics process. Peregrine *et al*. (1990) revealed the sequences that occur during the breakup of the drop in four stages, i.e., necking, bifurcation, recoil and secondary droplets.

Shi *et al*. (1994) show the effect of viscosity on the thread length during the drop formation process which was also investigated by Henderson *et al*. (1997). Zhang (1998) focuses on determining the effect of geometric parameters, physical properties and surface active materials on the dynamics of drop formation for low flow rate. They revealed that viscosity is the major stabilizing

Corresponding Author: Pardeep Bishnoi, National Institute of Technology, Department of Mechanical Engineering, Jamshedpur, 831014 Jharkhand, India

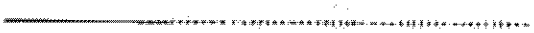

Fig. 1: Drop formation in savort's experiments

force. Tirtaatmadja *et al.* (2006) investigates the effect of molecular concentration on drop dynamic process and reveals that the material concentration has direct impact on the thread length means increased concentration increases the thread length as well as breakoff time period of the drop which was also studied by Drumright-Clarke and Renardy (2004).

Zhang *et al.* (1995) observed that surface tension forces the drop to be spherical. Surface tension is directly proportional to the detachment length of the pendent drop which was similar to the experimental study of Zhang (1999) who revealed the variation of break-off time as a function of surface tension. According to him, the accumulation time is fast if the capillary ratio (ε) is more. With a high capillary ratio, necking and detachment process keeps prolonged and deforms. For the stagnant value of viscosity ratio and variable value of the capillary ratio, breakoff length faintly depends on gravitational bond number (β). Grubelnik and Marhl (2005) experimentally revealed that the drop was formed near to the nozzle for a large surface tension liquid.

Zhang *et al.* (1997) also studied the effect of gravitational bond number on the drop formation. They observed that the drop volume decrease with an increase in the Gravitational bond number as per the relation $v_b \propto \beta^{-n}$ where, $n \approx 0.99$ which is analogous to Middleman (1995) and Zhang (1998). But for the higher value of gravitational bond number, no satellite drop formed which is observed by Zhang (1999).

Along with the impact of physical properties, operating conditions also influence the dynamics of drop formation. Zhang and Basaran (1995) observed that if we decrease the thickness of the capillary tube, elongation of the pendent drop increases while its volume decreases. But if the ratio of inner radius and outer capillary radius (R_i/R) is greater than 0.3, there is no impact of wall thickness on the drop dynamics. Similarly, the relative dimensionless drop elongation (Ld/R) rises as the radius of the tube increases. Chang *et al.* (2012) works experimentally on a silicone liquid says that drop's thread length decrease when we increase the capillary size. He validates this with his analytical solution. Zhang (1999) investigated the impact of wall thickness on drop formation. He said that for satellite drop formation, the value of wall thickness must be greater than 0.48.

Zhang *et al.* (1997) observed that for a fixed value of λ, β, ε increase in the external flow decrease the detachment volume which is similarly stated by Grubelnik and Marhl (2005). The external flow leads to the small-sized drops formation which was perceived by Clift *et al.* (1978). Zhang (1999) examined that if Reynolds number increases then thread length along with breakoff volume increases. Also, there is a transition between dripping to jetting occurs at high Reynolds number.

Beyond the experimental work, nowadays different numerical methods are used to examine the drop formation process. Dravid *et al.* (2008) observed the process of satellite drop formation and determine the conditions which required in controlling the diameter of drops. The Galerkin finite element approach is used to solve the governing equation. Pan and Suga (2003) investigates the pinch-off process of drop liquid into another liquid in a three-dimensional model. The level set method is used for the tracking of the complete pinch-off process. Renardy and Renardy (2002) develop an accurate representation of the body forces generated through surface tension and named it as the Parabolic Reconstruction of Surface Tension (PROST). The volume of fluid method is used for the solution of Navier-Stokes equation. Fawehinmi *et al.* (2005) studies the effect of flow rate and viscosity on the drop dynamic process through experiments and CFD packages, i.e., CFX and FLOW 3-D. Bishnoi *et al.* (2016a, b) investigate the effects of variation in operating parameters as well as design parameters on the satellite drop formation. The increase in both flow rate and diameter of nozzle inlet size leads towards more satellite droplet formation. Also, the impact of velocity variation on the smaller sized nozzle is less as compared to that of the large-sized nozzle.

The Volume of Fluid (VoF) is one of the commonly used methods. It is a free surface modeling technique for tracking and locating the free surface.

Current literature analyses the effect of various properties on the drop dynamic process. Available results explain the breakup process in a good manner but they did not provide the mathematical relation between thread length and various properties of the liquid at different liquid's concentration.

In this manuscript initially, the computational domain is verified with the literature results. Then, the variation of thread length due to viscosity and surface tension is demonstrated graphically and correlated through fitting curves techniques are being developed.

MATERIALS AND METHODS

Modelling, meshing, processing and simulation every task is done by using ANSYS fluent (14.0 Ver.). In all the cases, the models of the profile surface have been

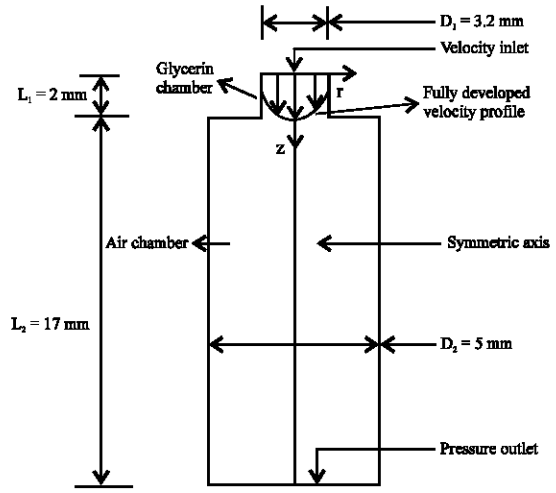

Fig. 2: Computational domain with different boundary condition's

generated, implicating the required boundary conditions. Geometric model of cuboid representing the system (drop) and the surrounding medium (atmospheric air) is modeled and meshed with a size sufficiently small such that the accuracy of the results obtained would be within the desired limit. The size of the system considered is such that accuracy of the result is not affected by it. After the breakoff of the first drop from the capillary tube, the residual liquid hanging from the tube takes the profile of a section of a sphere. All analysis is performed after the stability occurred.

Computational domain model with boundary conditions: The domain consists of two regions: a glycerin-85% chamber (capillary tube) and an air chamber with the coordinate system as shown in Fig. 2. The inside surface of the capillary is neutrally wettable while the surface surrounding the capillary orifice is non-wettable. We consider different compositions of glycerin as our base fluid which is being incompressible and Newtonian fluid as shown in Table 1. Flow velocity profile at the inlet is considered as fully developed. The outlet of the domain is considered as pressure outlet. To analyze the drop formation process from the capillary tube into ambient air, we use 'Volume of Fluid Model, i.e., VOF Model in the FLUENT Version 14.0.

At time zero, glycerin-85% fills the capillary tube, while the rest of the domain is filled with the air. Both fluids are assumed to be at rest. To initiate the ejection, the glycerin-85% velocity at the inlet boundary suddenly rises from 0-1 mL/min with fully developed profile and drops forms according to a gravitational law. Gravity force which acts towards Z-direction is also included in the simulation. Due to the axial symmetry of the problem, a two-dimensional geometry is used.

Mathematical modelling: For free surface flow, the detachment process of a drop depends on a lot of factors which include the velocity of drop liquid flow, the viscosity of liquid phase (μ), the density of both phases (ρ), the surface tension between liquid and air (σ) and the diameter of capillary tube.

The assumptions made in the mathematical formulation and the solution process are the following based on which the governing equations are written as:

- The fluid flows are Laminar and Newtonian
- The model is axisymmetric
- The surrounding air can be considered as incompressible
- The liquid properties are known and constant
- The evaporation of the liquid is neglected
- At the inlet of the capillary tube, fluid flow is assumed to be fully developed flow
- The thickness of the nozzle is neglected (Wilkes *et al*., 1999)

With the above assumptions, the Navier-Stokes equation in non-dimensional form for the transient motion of the liquid is given as:

$$\nabla.v = 0 \tag{1}$$

$$Re\left(\frac{\partial v}{\partial t}+v.\nabla v\right) = \nabla.\tau+\left(\frac{G}{Ca}\right)j \tag{2}$$

$$\tau = -pI+\left[\nabla v+(\nabla v)^{T}\right] \tag{3}$$

The variable in Eq. 1, i.e., Δ is the gradient operator; v is the resultant velocity vector. Similarly, in Eq. 2, τ is the stress tensor; j is the unit vector in the z-direction. In Eq. 3, p represents the dimensionless pressure and I is the identity tensor. Also during the non-dimensionalization process, three dimensionless numbers are introduced in Eq. 2:

- Reynolds number, $Re = \rho UD/\mu$
- Gravitational bond number, $G = \rho gR^2/\sigma$
- Capillary number, $Ca = \mu U/\sigma$

The flow is considered as fully developed, so, its velocity profile becomes:

$$v_z = \frac{2Q}{\pi R^2}\left\{1-\left(\frac{r}{R}\right)^2\right\},\ 0 \le r \le R \quad (4)$$

Where:
r = The radial coordinate of drop phase
v_z = The flow velocity in the Z-direction

The maximum velocity of liquid phase flow for the fully developed flow is given as:

$$U = \frac{2Q}{\pi R^2} \quad (5)$$

The tracking of the interface between two phases (i.e., pth and qth) is completed by solving a mass conservation equation for the volume fraction of one or more phases. The equation is as following for qth fluid:

$$\frac{1}{\rho_q\left[\frac{\partial}{\partial t}\left(a_q\rho_q\right)+\nabla\cdot\left(a_q\rho_q\vec{v}_q\right)=S_{\alpha_q}+\sum_{p=1}^{n}\left(\dot{m}_{pq}-\dot{m}_{qp}\right)\right]} \quad (6)$$

Where:
$\dot{m}_{pq}$ = The mass transfer from phase pth to phase qth
$\dot{m}_{qp}$ = The mass transfer from phase qth to phase pth

Generally, the source term, S_{α_q} on the right-hand side is zero. Only the volume fraction for the secondary phase fluid is solved. And the volume fraction of the primary phase fluid can be calculated by the following Eq. 7:

$$\sum_{p=1}^{n}\alpha_q = 1 \quad (7)$$

The boundary conditions for the solution of Eq. 1 and 2 which are also shown in Fig. 2 stated as:

- Inlet of the domain is velocity inlet
- Axis is considered as an axisymmetric axis
- Free slip velocity condition near the wall because the fluid near the wall is air
- Outlet of the computational domain is atmospheric pressure outlet

Grid generation: Grid generation is quite important work for the numerical analysis. The whole computational domain is divided into several numbers of cells. The cell arrangement in the nozzle within the domain is shown in Fig. 3. It can be marked that the cell density is too dense near the axisymmetric axis as compared to the remaining domain because the detachment profile of drop formation moves along the axis of the domain. It means a zone

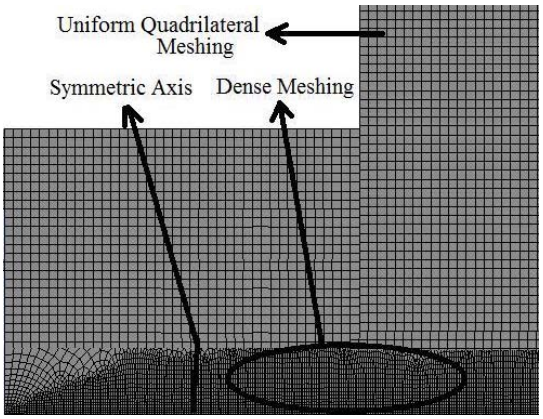

Fig. 3: Schematic diagram of grid generation in the computational domain

nearby axisymmetric axis is the main area for the analysis. The cells are quadrilateral in shape throughout the domain. The development of the detachment profile of the pendent drop occurs near the axisymmetric axis, so, the smaller cells are placed near the axis.

Numerical solution procedure: Meshing plays an important role in the numerical solutions obtained through the computational methods. More is the number of cells; the much accurate result can be obtained. Geometric models have meshed with a sufficiently small size such that the accuracy of the results obtained would be within the desired limit. The bounding surfaces of the system have been defined by names and the top surface has been defined as open to atmosphere. An unsteady pressure-based solver, using laminar flow model has been adopted with gravity assigned acting towards Z directions. A User-Defined Function (UDF) source code for the fully developed flow was invoked and interpreted using the interpreter and was hooked to boundary conditions. The zones representing the two phases were marked and the material properties were assigned by patching. The nature of the movement of the drop was studied. FLUENT Version 14.0 used a grid solver which solves the Navier-Stokes equations in an iterative manner by applying the above-mentioned boundary conditions. Pressure Implicit with Splitting of Operators (PISO) algorithm along with PREssure STaggering Option (PRESTO) scheme is used for the discretization process. Under-relaxation factor for pressure is 0.3 and that for momentum is 0.7 were used for the convergence of all variables. In general, regular quadrilateral cells were used for the entire computational domain. The convergence of the discretized equations was said to have been achieved when the whole field residual for all the variables fell below 10^{-3} for u, v.

RESULTS AND DISCUSSION

Grid sensitivity test: As per the numerical solution procedure, the meshing should be fine but it will increase the time period of the whole computational process. The basic purpose of grid sensitivity test is to determine the accuracy of the computational results for different meshing conditions. In VOF approach path profile of the moving drop is located. If meshing is poor, then the location of the liquid drop is not so accurate as compared to higher one. In this computational work, 8,000, 30,000 and 50,000 cells grid sized meshing is analyzed. Figure 4 demonstrates the meshing having 8,000 and 30,000 cells.

As shown in Fig. 4, the free surface of drop profile for the dense mesh is better to locate as compared to the lighter mesh size. For the further computation, 30,000 cells meshing are considered better than 8,000 in tracing the free surface and efficient than 50,000 cells in overall computational time.

Comparison of drop detachment profile with experimental result: Figure 5 shows the comparison of different sequences of drop formation obtained from the experimental method (Wilkes *et al*., 1999) and VOF numerical method. The actual detachment time of the 85% glycerin drop in the air is 5.07 sec (from initial) and 2.29 sec (after previous drop's detachment) which is within 3% error as compared with the Wilkes *et al*. (1999). Furthermore, the above image proves that the VOF method also provides the precise information regarding the motion of drop during the detachment process.

Drop elongation and breakup: On the valid computational domain, now, we screen out the variations of the dimensionless thread length at various flow rates with respect to the detachment time period, i.e., t_d-t as shown in Fig. 6.

When the flow rate increases, the thread length of the drop before the detachment increases whereas the time period of the detachment decreases. The value of dimensionless drop elongation just before the detachment is more with low flow rate as compared to higher flow rate. The reason behind this is that at high flow rate pendant drop lost its equilibrium prior to low flow rate. The liquid flow rate also toughens the occurrence of drop fabrication. A similar development is also reported by Zhang *et al*. (1995).

Figure 7 demonstrates the variation of the dimensionless minimum radius of the thread a/R and the dimensionless drop elongation L/R with comparative detachment time (t_d- t) for 85% glycerin developing out of

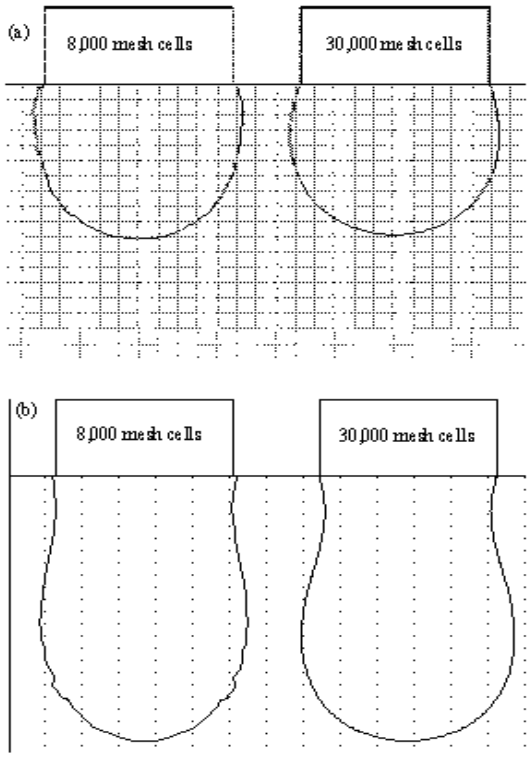

Fig. 4: Grid sensitivity test: a) 1.50 sec and b) 3.0 sec

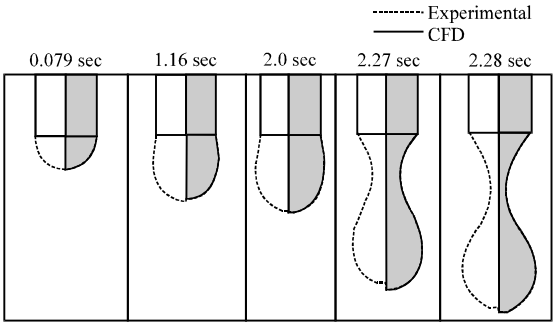

Fig. 5: Comparison of detachments profile of pendent drop at various time sequences for experimental and computational methods

a capillary tube of R = 1.6 mm at Q = 1 mL/min. It proves that the viscosity plays a crucial role during the necking and breakup dynamics of forming drops. Also, the thread length of the breakoff drop elongates and the width of the liquid thread becomes constantly decreases as the time period proceeds until it reaches breakoff.

Influence of viscosity on drop dynamics process: As per Kumar and Kuloor (1970), there is a marginal variation of viscosity on the volume of the detached drop. However,

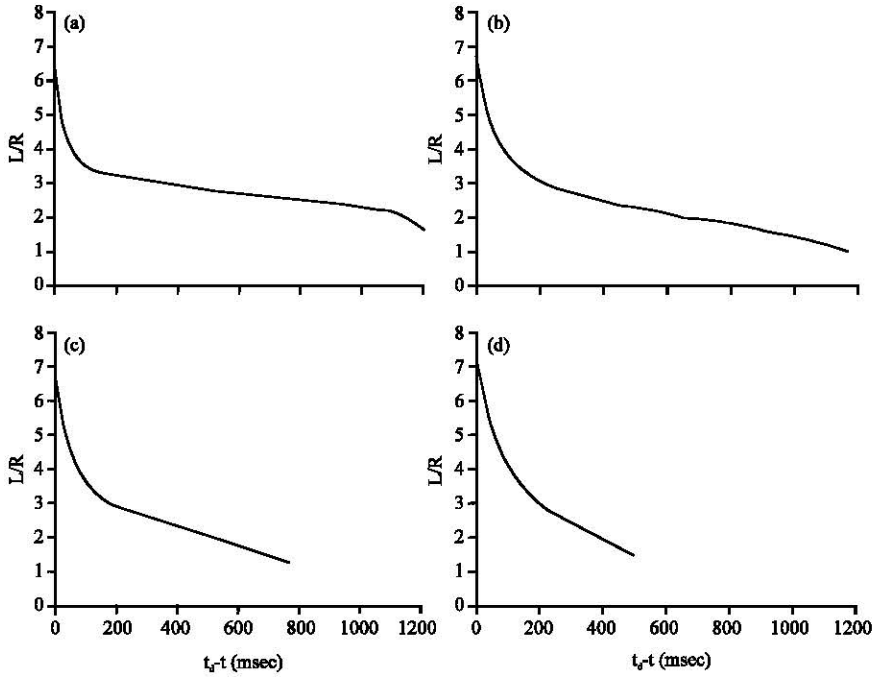

Fig. 6: Variation of dimensionless thread length with detachment time period for different flow rate: a) 1 mL/min; b) 2 mL/min; c) 3 mL/min and d) 4 mL/min

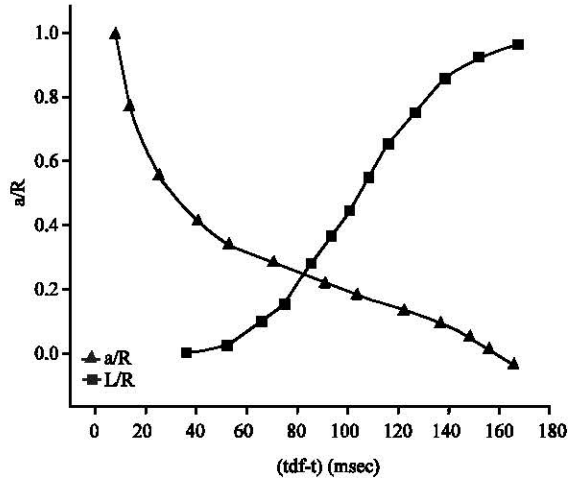

Fig. 7: Variation of dimensionless thread length with dimensionless minimum thread radius with detachment time

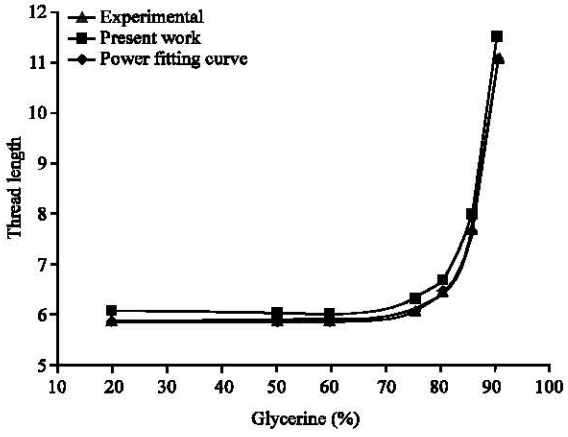

Fig. 8: Variation of thread length as a function of different glycerin compositions

it actively influences the drop formation process, especially during necking and breakoff time period. The impact of viscosity on the thread length for the different composition of glycerine is plotted in Fig. 8. The viscosity of the liquid is an important parameter to curb the interfacial undulations of the breakoff drop. It smoothens the detachment profile of the drop at every stage before breakoff.

When we compare the spring balance system with the drop dynamic system, then the viscosity of the liquid used in the drop process plays the similar character as damping force plays in the spring balance system. The increase in viscosity of the liquid will eliminate the oscillation that occurs during drop formation process and also increases the breakoff period of the process.

Figure 8 shows the thread length's dependency on the percentage glycerine composition. The limit of

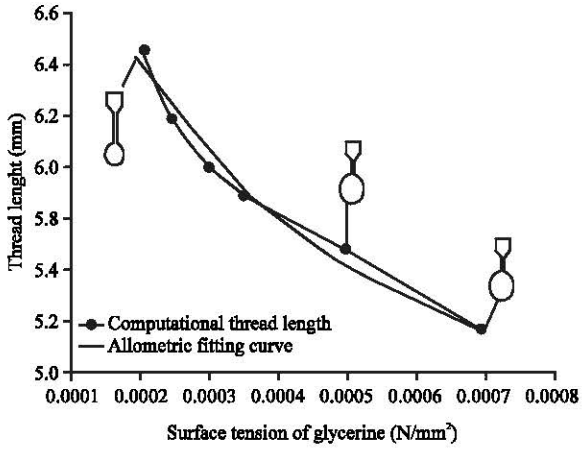

Fig. 9: Variation of thread length as a function of surface tension of glycerine

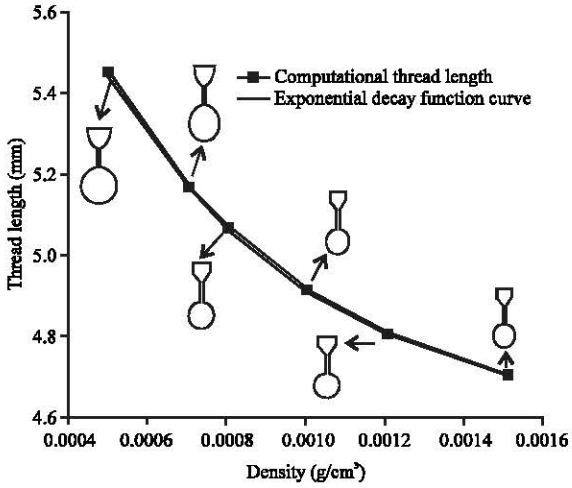

Fig. 10: Variation of thread length as a function of density of the glycerine

glycerine composition is varying from 0-100%. Thread length is increasing exponentially with the increasing percentage content of the glycerine. The percentage content of the glycerine of thread length was manifested in all the samples of glycerine. The percentage content of the glycerine dependence upon the thread length is fitted using Power model as shown in Eq. 8. Relation shown in Eq. 8, exist only on the initial boundary conditions of the system. The value of the coefficient of determination for the fitted curve is 0.99984 which represent the best regression curve for the data. The given Eq. 8 is valid for Q = 1 mL/min and the values of glycerine viscosity at different compositions used in the computational analysis that is shown in Fig. 8.

$$L_i = 5.43914 + 4.048e^{-36} \times C_i^{18.49} \quad (8)$$

Where:

L_i = Thread length (mm)

C_i = Different percentage age glycerine composition

Influence of surface tension on drop dynamics process: Figure 9 shows the variation of surface tension by keeping density and viscosity constant. The sequence of the drop's shown is 1 m sec before the detachment period.

Surface tension is the basic force due to which the liquid drop adopts the spherical shape near the capillary tip. The surface tension force plays a critical role in manipulating the behavior of the detachment droplets. The drop at the needle is gripped by the interfacial tension force, due to which the time taken for the equilibrium of forces is less for systems with lower interfacial tension. Surface tension shows the mutual interactions of the liquid volume. Higher the surface tension indicates the more cohesive power of the liquid. Due to this reason with an increase of surface tension the following happens:

- Increase in the size of the pendent drop
- Decrease in the thread length as shown in Fig. 9
- Increase in the breakup time of the pendent drop

To determine the relationship between thread length and surface tension, the allometric curve is selected as the best fit curve for the computational variation. The value of the coefficient of determination is 0.9869 for the regression. Equation 9 represents the relation between thread length and different values of the glycerine's surface tension:

$$L_i = 1.56263 \times \sigma_i^{-0.16511} \quad (9)$$

Where:

L_i = Thread length (mm)

σ_i = Various surface tension values (N/mm^2)

Influence of density on drop dynamics process: Figure 10 shows the variation of density on the detachment profile of the pendent drop by keeping surface tension and viscosity constant. Given variation shows that with a decrease in the density of the pendent drop liquid, the breakoff volume of the drop increases. As we say that a more dense body has more weight which means more gravitational pull is exerted on the pendent drop. So, for high-density value and due to more pulling force, the pendent drop detaches earlier as compared to the other ones. Also, the thread length of the high-density liquid

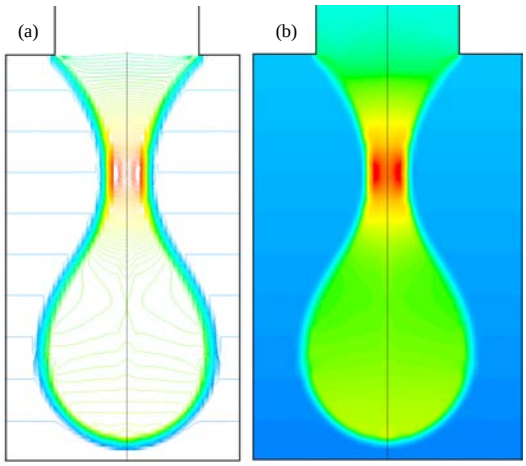

Fig. 11: Pressure contour of glycerin drop profile

pendent drop is small as well as the satellite drop formation will not occur with the value of density being high. Equation 10 shows the dependence curve of thread length upon the density of the liquid. The curve having exponential decay function superlatively fits the computational domain thread length curve as shown in Fig. 10. The value of the coefficient of determination is 0.999886 which indicates a perfect fit of the exponential decay function curve with the computational results. Equation 10 is valid for Q = 1 mL/min and the values of density used in the computational analysis that is shown in Fig. 10:

$$L_i = 2.48446 \times \frac{\rho_i}{e^{5.2389e^{-4}}} + 4.479 \quad (10)$$

Where:

L_i = Thread length (mm)

ρ_i = The various density values (g/cm^3)

Study of pressure contour profile: Figure 11 shows the variation of pressure within the droplet region. The value of pressure is more at the neck region as compared to the other zones of the drop. The region behind this is that a stagnation point is generated at the midpoint of necking region. Now, the fluid is driving in the upstream and downstream directions with respect to the stagnation point. The fluid that is moving upstream blocks the inlet flow of the liquid. Due to this high-pressure zone, the further inflow of liquid in the drop is terminated.

CONCLUSION

To study the parametric effects on the dynamics of drop formation, a computational domain is being developed and verified it with the experimental model available in the literature. As the best computational way to study the free surface problems is volume of fluid method, so is used for the numerical simulation to locate the surface of drop during and after the breakoff process. Viscosity plays an impactful role in stabilizing the drop during the detachment process. Also, Viscosity directly affects the breakoff thread length of the drop. For a low value of viscosity, thread length variation is negligible whereas for high viscosity liquids, thread length varies exponentially with viscosity. This increase in thread length also increases the chances of satellite drop formation. When the flow rate increases, dimensionless thread length also increases while the detachment time period decreases.

It is also revealed that the increase in density will decrease the thread length as well as droplet volume. In a similar way if we increase the surface tension, the breakup volume of the droplet increases while the thread length of the drop decreases because the cohesive force of the liquid directly depends on the surface tension. If we increase the surface tension, cohesive force between the liquid molecules increases which increases the volume of the droplet while its thread length variation is negligible as compared to that of volume change. This analysis also revealed that at the necking zone, the value of pressure is being the maximum as compared to the other regions of the drop detachment profile.

RECOMMENDATIONS

This investigation also proves that the CFD tools are quite efficient, accurate for the free surface flow problems. Furthermore, the above result proves that the VOF method also provides the precise information regarding the motion of drop during the detachment process.

REFERENCES

Basaran, O.A., 2002. Small-scale free surface flows with breakup: Drop formation and emerging applications. AIChE. J., 48: 1842-1848.

Bhat, P.P., 2008. Drop formation: Methods and applications. Master Thesis, Purdue University, West Lafayette, Indiana.

Bishnoi, P., D. Patel, M. Srivastava and M.K. Sinha, 2016a. CFD analysis of the factors affecting the Satellite drop formation. Intl. J. Adv. Res. Sci. Eng., 5: 707-713.

Bishnoi, P., D. Patel, M. Srivastava and M.K. Sinha, 2016b. CFD analysis of the factors affecting the Satellite drop formation. Intl. J. Adv. Res. Sci. Eng., 5: 707-713.

Calvert, P., 2007. Printing cells. Sci., 318: 208-209.

Chang, B., G. Nave and S. Jung, 2012. Drop formation from a wettable nozzle. Commun. Nonlinear Sci. Numer. ySimul., 17: 2045-2051.

Clift, R., J.R. Grace and M.E. Weber, 1978. Bubbles, Drops and Particles. 3rd Edn., Academic Press, Cambridge, Massachusetts, USA., ISBN:9780121769505, Pages: 380.

Doring, M., 1982. Ink-jet printing. Philips Tech. Rev., 40: 192-198.

Dravid, V., P.B. Loke, C.M. Corvalan and P.E. Sojka, 2008. Drop formation in non-Newtonian jets at low Reynolds numbers. J. Fluids Eng., 130: 1-8.

Drumright-Clarke, M.A. and Y. Renardy, 2004. The effect of insoluble surfactant at dilute concentration on drop breakup under shear with inertia. Phys. Fluids, 16: 14-21.

Eggers, J., 1997. Nonlinear dynamics and breakup of free-surface flows. Rev. Mod. Phys., 69: 865-930.

Fawehinmi, O.B., P.H. Gaskell, P.K. Jimack, N. Kapur and H.M. Thompson, 2005. A combined experimental and computational fluid dynamics analysis of the dynamics of drop formation. Proc. Inst. Mech. Eng. Part C. J. Mech. Eng. Sci., 219: 933-947.

Grubelnik, V. and M. Marhl, 2005. Drop formation in a falling stream of liquid. Am. J. Phys., 73: 415-419.

Hauser, E.A., H.E. Edgerton, B.M. Holt and J.T. Cox Jr, 1936. The application of the high-speed motion picture camera to research on the surface tension of liquids. J. Phys. Chem., 40: 973-988.

Henderson, D.M., W.G. Pritchard and L.B. Smolka, 1997. On the pinch-off of a pendant drop of viscous fluid. Phys. Fluids, 9: 3188-3200.

Kumar, R. and N.R. Kuloor, 1970. Bubble formation in viscous liquids under constant flow conditions. Can. J. Chem. Eng., 48: 383-388.

Middleman, S., 1995. Modeling Axisymmetric Flows: Dynamics of Films, Jets and Drop. ASEE, New York, USA., Pages: 299.

Pan, Y. and K. Suga, 2003. Capturing the pinch-off of liquid jets by the level set method. J. Fluids Eng., 125: 922-927.

Peregrine, D.H., G. Shoker and A. Symon, 1990. The bifurcation of liquid bridges. J. Fluid Mech., 212: 25-39.

Rayleigh, L., 1878. On the instability of jets. Proc. London Math. Soc., 1: 4-13.

Rembe, C., J. Patzer, E.P. Hofer and P. Krehl, 1996. Realcinematographic visualization of droplet ejection in thermal ink jets. J. Imaging Sci. Technol., 40: 400-404.

Rembe, C., M. Beuten and E.P. Hofer, 1999. Investigations of nonreproducible phenomena in thermal ink jets with real high-speed cine photomicrography. J. Imaging Sci. Technol., 43: 325-331.

Renardy, Y. and M. Renardy, 2002. PROST: A parabolic reconstruction of surface tension for the volume-of-fluid method. J. Comput. Phys., 183: 400-421.

Savart, F., 1833. Treatise on constitution of the liquid flow jetted out through orifice of thin plate. Ann. Chem., 53: 337-386.

Shi, X.D., M.P. Brenner and S.R. Nagel, 1994. A cascade of structure in a drop falling from a faucet. Sci., 265: 219-222.

Sirringhaus, H., T. Kawase, R.H. Friend, T. Shimoda and M. Inbasekaran *et al*., 2000. High-resolution inkjet printing of all-polymer transistor circuits. Sci., 290: 2123-2126.

Stone, H.A., B.J. Bentley and L.G. Leal, 1986. An experimental study of transient effects in the breakup of viscous drops. J. Fluid Mech., 173: 131-158.

Tirtaatmadja, V., G.H. McKinley and J.J. Cooper-White, 2006. Drop formation and breakup of low viscosity elastic fluids: Effects of molecular weight and concentration. Phys. Fluids, 18: 1-18.

Tjahjadi, M.S.H.A., H.A. Stone and J.M. Ottino, 1992. Satellite and subsatellite formation in capillary breakup. J. Fluid Mech., 243: 297-317.

Wehking, J.D., M. Gabany, L. Chew and R. Kumar, 2014. Effects of viscosity, interfacial tension and flow geometry on droplet formation in a microfluidic T-junction. Microfluid. Nanofluid., 16: 441-453.

Wilkes, E.D., S.D. Phillips and O.A. Basaran, 1999. Computational and experimental analysis of dynamics of drop formation. Phys. Fluids, 11: 3577-3598.

Zhang, D.F. and H.A. Stone, 1997. Drop formation in viscous flows at a vertical capillary tube. Phys. Fluids, 9: 2234-2242.

Zhang, X. and O.A. Basaran, 1995. An experimental study of dynamics of drop formation. Phys. Fluids, 7: 1184-1203.

Zhang, X., 1999. Dynamics of drop formation in viscous flows. Chem. Eng. Sci., 54: 1759-1774.Zhang, X., 1999. Dynamics of growth and breakup of viscous pendant drops into air. J. Colloid Interface Sci., 212: 107-122.